Effects of Monomer Functionality and Hydrogen Bonding on the Polymerization Kinetics and Properties of Thiol−Ene Networks

Hui Zhou, Qin Li, Junghwan Shin, and Charles E. Hoyle*

School of Polymers and High Performance Materials, The University of Southern Mississippi, Hattiesburg, Mississippi 39406

Received November 25, 2008; Revised Manuscript Received February 17, 2009

ABSTRACT: The effect of hydrogen bonding on both the kinetics and physical properties of photopolymerized thiol−ene systems has been determined by comparison of two thiol−ene systems, [butyl 3-mercaptopropionate/pentaerythritol tetrakis(3-mercaptopropionate)]/triallyl-1,3,5-triazine-2,4,6(1*H*,3*H*,5*H*)-trione and [3-mercaptopropionic acid/pentaerythritol tetrakis(3-mercaptopropionate)]/triallyl-1,3,5-triazine-2,4,6(1*H*,3*H*,5*H*)-trione. Hydrogen bonding in the thiol−ene network incorporating 3-mercaptopropionic acid leads to enhanced glass transition temperatures, refractive index, Persoz hardness, elastic modulus values, isothermal enthalpic relaxation, and rubbery−glassy heat capacity differences compared to networks formed using butyl 3-mercaptopropionate. Sub-T_g aging analysis clearly shows that hydrogen bonding affects the isothermal enthalpic relaxation process.

Introduction

Hydrogen bonding is a critical factor in determining the physical and mechanical properties of many polymeric materials. For example, it has been reported that inter- and intramolecular hydrogen-bonding interactions have been used to alter the miscibility between polymers containing hydrogen bond donors and acceptors.[1−5] These studies, however, have mainly focused on polymer hydrogen bonding in blends, bulk, and solution. Recently, there has been considerable attention dealing with hydrogen-bonding effects on photopolymerization kinetics of a wide variety of acrylate monomers by Jansen et al.[6] and Bowman et al.[7,8] Jansen et al.[6] found that acrylates with urethane and amide side groups capable of hydrogen bonding exhibited very fast polymerization rates at room temperature. However, at high temperatures the rates decreased along with a reduction in the extent of hydrogen bonding measured by infrared analysis. Additionally, the polymerization of hydroxyalkyl acrylates and acid-containing (meth)acrylate monomers has been investigated by examining the extent of hydrogen bonding before and during polymerization.[9,10] Despite the recent reports on hydrogen-bonding effects on linear polymer and lightly cross-linked polymers, no attention has been paid to hydrogen-bonding impact on the kinetics of photopolymerization and the physical and mechanical properties of pure highly cross-linked network films. Since photopolymerized thiol−enes form highly uniform networks, they present an outstanding molecular platform to use in delineating the effect that hydrogen bonding has on the kinetics of network formation and the resulting network properties.

In the present study, we extend our previous investigation[9,10] of hydrogen-bonding effects on acrylate polymerization leading to linear polymers to thiol−ene photopolymerization which produces networks. Thiol−ene polymerization proceeds via a step-growth free-radical chain process resulting in the formation of networks, as we have already noted, with unprecedented uniformity based on dynamic mechanical analysis and differential scanning calorimetric analysis.[11−13] This affords a distinct and heretofore unexploited opportunity to evaluate the effect of hydrogen bonding on free-radical step-growth kinetics as well as the effect of hydrogen bonding on thermal transitions and basic physical and mechanical network properties.

Table 1. Calculation of Thiol Average Functionality (TAF) of Thiol Mixture

$[SH]_{Tetra\ Thiol}$:$[SH]_{Mono\ Thiol}$	$M_{Tetra\ Thiol}/M_{Mono\ Thiol}$	TAF[a]	gel point (%)[b]
100:0		4.00	40.8
95:5	4.75	3.48	44.9
90:10	2.25	3.08	49.0
80:20	1.00	2.50	57.7
65:35	0.46	1.95	72.6
50:50	0.25	1.60	91.3

[a] $TAF = (M_{Tetra\ Thiol} \times 4 + M_{Mono\ Thiol} \times 1)/(M_{Tetra\ Thiol} + M_{Mono\ Thiol})$. [b] Calculated from the reaction with TTT.

Experimental Section

Materials. Trimethlolpropane tris(3-mercaptopropionate) (Tri Thiol) and pentaerythritol tetrakis(3-mercaptopropionate) (Tetra Thiol) were obtained from Bruno Bock Chemische Fabrik GmbH & Co. KG and used as received. Butyl 3-mercaptopropinate (BMP), 3-mercaptopropionic acid (MPA), and triallyl-1,3,5-triazine-2,4,6(1*H*,3*H*,5*H*)-trione (TTT) were obtained from Aldrich and used as received (Scheme 1). 2,2-Dimethoxy-2-phenylacetophenone (DMPA) was obtained from Ciba Specialty Chemicals Corp. and used as received.

Sample Preparation and Characterization. Sample mixtures were prepared according to recipes in Table 1. It should be noted that the Tetra Thiol and Tri Thiol samples are not exactly four and three functional as some impurities are present in each. For the work reported herein, it is assumed that the functionalities are three

Scheme 1. Tri Thiol, Tetra Thiol, Monothiols (BMP and MPA), and Ene (TTT)

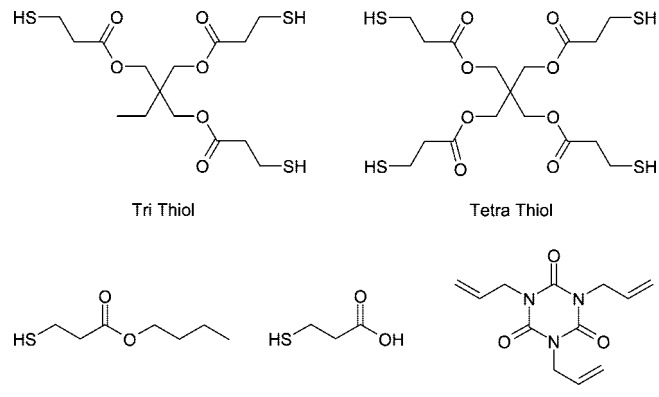

* Corresponding author. E-mail: Charles.Hoyle@usm.edu.

10.1021/ma802645j CCC: $40.75
Published on Web 03/30/2009

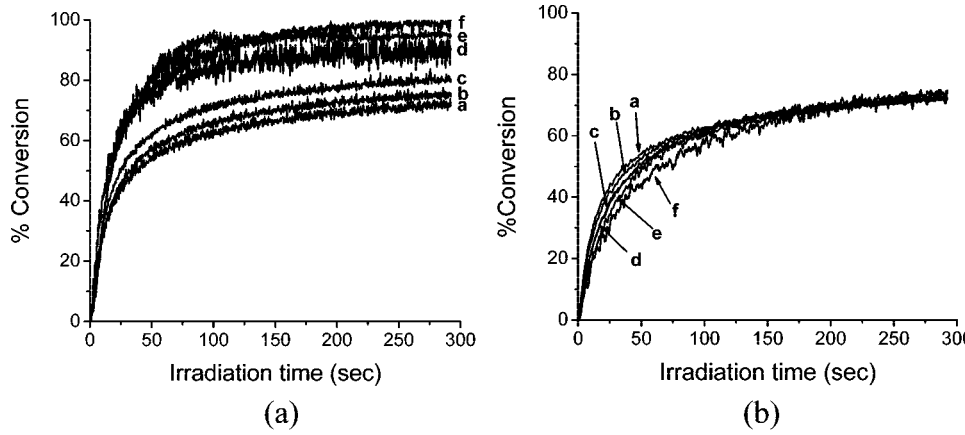

Figure 1. Conversion vs time as determined via RTIR for (a) (BMP/Tetra Thiol)/TTT and (b) (MPA/Tetra Thiol)/TTT system. Molar ratio of Mono Thiol/Tetra Thiol: (a) 0:100, (b) 5:95, (c) 10:90, (d) 20:80, (e) 35:65, and (f) 50:50. Results are for ene conversion at 3080 cm^{-1}. Light intensity is 0.55 mW/cm^2.

(Tri Thiol) and four (Tetra Thiol) for the purpose of estimating thiol average functionality (TAF) values. However, this does not change any of the conclusions drawn from the results. Finally, the thiol mixtures were combined with TTT (1:1 molar ratio based on functionality) to form the photocurable thiol−ene systems investigated. Real-time infrared (RTIR) spectra were recorded on a modified Bruker 88 spectrometer. UV light from an Oriel lamp system equipped with a 200 W, high-pressure mercury−xenon bulb was channeled through an electric shutter and fiber-optic cable in the sample chamber. Photopolymerizations were conducted in a cell prepared by sandwiching the samples between two sodium chloride salt plates at a thickness of ~20 μm using a light intensity of 0.55 mW/cm^2 measured with an IL-1400 calibrated radiometer from International Light. Infrared absorption spectra were obtained under continuous UV irradiation at a scanning rate of 5 scans/s. 1 wt % photoinitiator (DMPA) was used in each sample. The characteristic infrared absorbance bands used to monitor the disappearance of the reactant and monomer during the photoreactions were as follows: ene at 3080 cm^{-1} and thiol at 2570 cm^{-1}. The results for both thiol and ene conversion were essentially identical so plots are only given for the ene conversion in Figure 1. The reactant conversions, as calculated from the change in the peak area over time, have an approximate error of ±2%.

To prepare films, thiol−ene coatings on glass plates prepared by using a 125 μm draw down bar on glass were exposed for 10 passes to the output of a Fusion high-intensity lamp system with conveyer belt. The lamp system was equipped with a D bulb (400 W/in. input) with line speed of 3.05 m/min and irradiance of 3.0 W/cm^2. Films were evaluated by DSC, refractive index analysis, and Persoz hardness measurements. Persoz pendulum hardness (ASTM D-4366 using a BYK-Gardner pendulum hardness tester with a square frame pendulum) values were the average of six tests. DSC measurements were conducted on a DSC Q 1000 TA Instruments under nitrogen at a heating and cooling rate of 10 °C/min. For sub-T_g isothermal annealing experiments, typically, a sample was heated to (T_g + 50) °C to eliminate any thermal history, then cooled down to (T_g − 10) °C and maintained at this temperature, and then further cooled down to (T_g − 50) °C. Finally, the sample was heated to (T_g + 50) °C and the scan recorded. To obtain comparison data without the isothermal annealing, the sample also was heated to 150 °C and then cooled down to (T_g − 50) °C directly, before heating to (T_g + 50) °C while recording the DSC heating scan. The dynamic mechanical spectra were obtained on a TA Q800 DMA (TA Instruments) operating at 1 Hz and a heating rate of 3 °C/min (tensile mode). The refractive index was obtained using a Bausch&Lomb ABBE-3 L refractometer at 24 °C. 1-Bromonaphthalene was applied between the sample film and the prism shield. Acetonitrile, which has a high dielectric constant, was used to measure the gel fraction of the photocured thiol−ene films. The gel fraction was calculated as the weight difference between the initial weight and the weight of films after extraction in acetonitrile at 65 °C for 5 days.

Results and Discussion

The monomers used in the investigation are shown in Scheme 1. 3-Mercaptopropionic acid (MPA) and butyl 3-mercaptopropionate (BMP) were used as monothiol monomers with and without hydrogen-bonding capability, respectively. Triallyl-1,3,5-triazine-2,4,6(1*H*,3*H*,5*H*)-trione (TTT) was selected as the trifunctional ene monomer. Two thiol−ene systems were evaluated: (BMP/Tetra Thiol)/TTT and (MPA/Tetra Thiol)/TTT. Different amounts of the two monothiol monomers, MPA and BMP, were mixed with Tetra Thiol to obtain thiol mixtures with different thiol average functionality (TAF): the TAF values are listed in Table 1. All components were soluble over the concentration range evaluated. A kinetic analysis of the polymerization was first conducted to ascertain the effect of the acid functional groups in the MPA thiol on the thiol−ene polymerization rate. This was followed by physical characterization of the subsequent networks. The effect of hydrogen bonding on thermal, mechanical, and optical properties of the thiol−ene films was evaluated accordingly.

Kinetics. The monofunctional thiol monomer, with/without hydrogen-bonding capability, can potentially change the polymerization kinetics as well as the physical and mechanical properties of the thiol−ene cured networks. Real-time polymerization results shown in Figure 1a,b indicate significantly different kinetics for the two systems. With an increase of the concentration of BMP and corresponding decrease in the TAF (as shown in Table 1), the conversion of thiol and ene increased (see results in Figure 2) while the matrix density decreased. However, the extent (Figure 2) or rate of conversion of thiol and ene (Figure 1a) did not change with increasing MPA (with hydrogen-bonding capability) concentration. Because of hydrogen bonding afforded by the acid groups in MPA, MPA actually acts as a pseudo-multifunctional thiol, and hence the rate and extent of conversion do not measurably decrease to an appreciable extent as the concentration of MPA increases. To illustrate the presence of the hydrogen bonding in the (MPA/Tetra Thiol)/TTT network, infrared spectra were recorded for (MPA/Tetra Thiol)/TTT and (BMP/Tetra Thiol)/TTT network films. The results in Figure 3 clearly show the presence of hydrogen bonding as exhibited by the very broad hydroxyl peak around 3200 cm^{-1} due to hydrogen bonding of acid groups. It is noted that there were also changes in the IR spectrum in the carbonyl region. However, because of the presence of multiple carbonyls, a comprehensive analysis of the hydrogen bonding

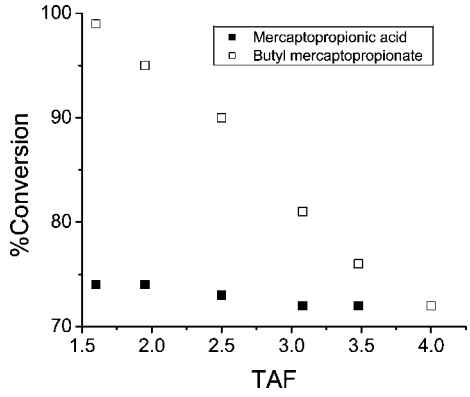

Figure 2. Conversion as a function of thiol average functionality (TAF) obtained from plots in Figure 1.

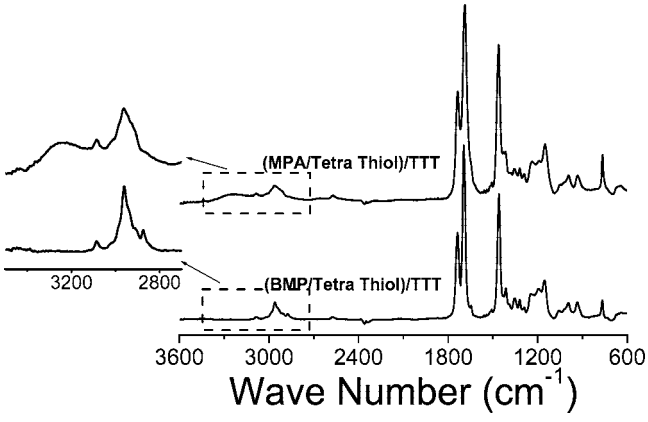

Figure 3. IR spectra for (MPA/Tetra Thiol)/TTT and (BMP/Tetra Thiol)/TTT. Molar ratio of MPA or BMP/Tetra Thiol is 35:65.

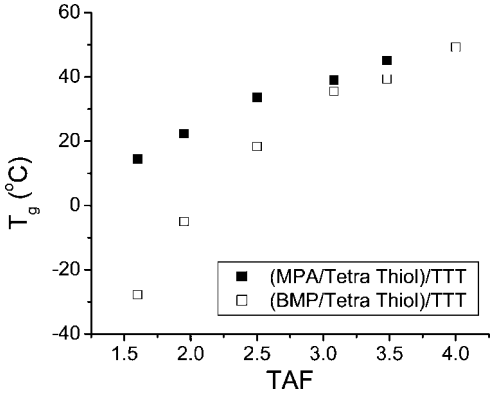

Figure 4. T_g as a function of thiol average functionality (TAF) for (MPA/Tetra Thiol)/TTT and (BMP/Tetra Thiol)/TTT films by DSC.

in the carbonyl region around 1675−1730 cm^{-1} was not attempted.

Thermal, Optical, and Physical Analysis. Next, thiol−ene-based films were prepared for physical, mechanical, and optical analysis. It should be noted that much higher light intensities and significantly larger total doses than used for the kinetic analysis in Figure 1 were employed to cure the thiol−ene films used for property evaluation. In this way, high conversions are obtained in each case, giving films suitable for assessment and comparison. DSC data in Figure 4 show that in both types of photopolymerized thiol−ene systems the T_g decreases with increase of the monothiol monomer content. It is clear to see that the T_gs are quite different for a given TAF for the two systems. The differences in T_g between systems containing MPA and BMP can be as high as 42 °C when the TAF is 1.60 (see Figure 4). Of course, as TAF increases, the incremental increase in T_g due to hydrogen bonding by the networks incorporating MPA diminishes as the inherent chemical based network cross-link density increases. Nonetheless, it can be concluded that hydrogen bonding provided by MPA leads to higher T_g values for all of the (MPA/Tetra Thiol)/TTT systems.

Dynamic mechanical measurements were also conducted for both systems (Figure 5); results for 50:50 (MPA:TetraThiol)/TTT and (BMP:TetraThiol)/TTT samples are not given since the sample integrity for the (BMP:TetraThiol)/TTT based network did not allow for reproducible measurement. With the decrease of TAF, both MPA and BMP containing systems exhibit glass transition shifts to lower temperature as a result of a decrease in network linking density, i.e., cross-link density (Table 2). An increase in tan δ peak height with a decrease in TAF implies better energy damping of the network corresponding to the temperature at which the peak maximum occurs. Similar to the DSC measurements, hydrogen bonding also leads to higher T_g values for systems containing a given concentration of reacted MPA compared to comparable BMP containing systems. Concentrating on the storage modulus (E') in the rubbery plateau taken from Figure 5 and listed in Table 3, it is obvious that as the concentration of BMP or MPA increases, the modulus decreases, no doubt the result of a decrease in the network cross-link density. Interestingly, for essentially any given concentration of BMP or MPA, the modulus at $T_g + 50$ °C is greater for the film prepared with MPA as the monofunctional thiol. This is a direct result of the increase in network cross-link density afforded by the physical hydrogen bonding provided by the carboxylic acid groups.

Refractive index, an important parameter for optical applications, is directly related to density and the polarizability of the repeat unit.[14] Consider the two systems in this study. The refractive index drops substantially (Figure 6) for the (BMP/Tetra Thiol)/TTT based networks as the TAF decreases and the network linking density decreases. However, for the (MPA/Tetra Thiol)/TTT networks, the refractive index does not measurably change (Figure 6) with increasing MPA concentration, probably due in part to the increased hydrogen bonding when MPA is used compared to BMP.

Results shown in Figure 7 indicate that in both types of photopolymerized networks Persoz hardness decreases with an increase of monothiol monomer content. For the (BMP/Tetra Thiol)/TTT systems, when the thiol average functionality is less than 2.5, the polymer films are not suitable for Persoz hardness measurements. In these cases, the films are very soft and the thickness is difficult to control due to the lower viscosity for systems with higher BMP concentration. For (MPA/Tetra Thiol)/TTT systems, the cured films were of high quality due to strong hydrogen bonding in the network. Even with large amounts of MPA, films prepared from samples with TAF less than 2.5 are uniform and have thicknesses comparable to films made from samples where the TAF is between 2.5 and 4.0, allowing for accurate assessment of Persoz pendulum hardness.

In order to place the results for (BMP/Tetra Thiol)/TTT and (MPA/Tetra Thiol)/TTT systems in a proper frame of reference, a base system comprised of a 1:1 molar functional group mixture of Tri Thiol/TTT was photocured, and the corresponding glass transition, pendulum hardness, and refractive index were obtained. Comparisons of thermal, optical, and mechanical data for the three thiol−ene networks, which have about the same TAF, are shown in Tables 4 and 5. It is interesting to note that the (BMP/Tetra Thiol)/TTT network with TAF of 3.08 has physical properties similar to those for the pure 1:1 Tri Thiol/TTT based network (Table 4). In contrast, because of hydrogen bonding, even though the (MPA/Tetra Thiol)/TTT network has the same thiol average functionality, the glass transition tem-

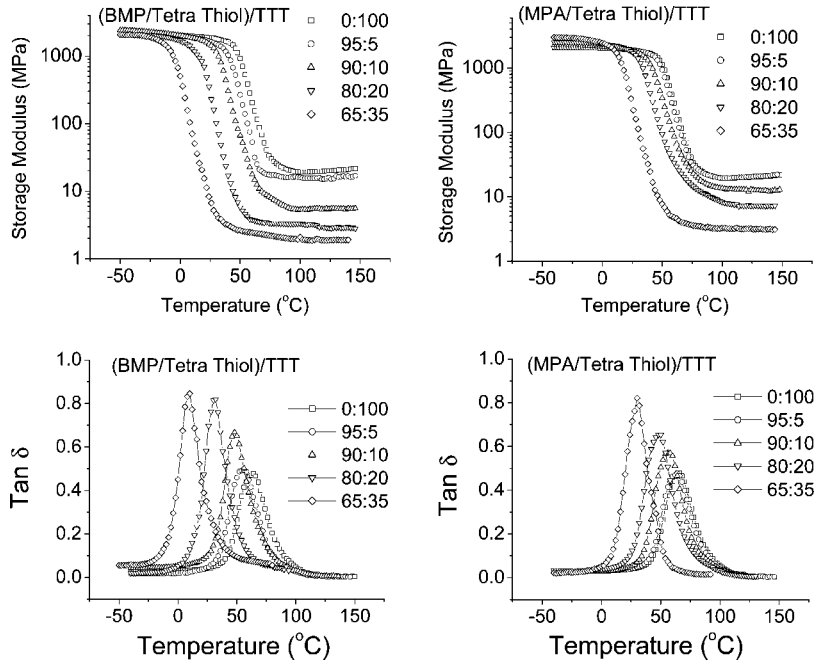

Figure 5. Storage modulus and tan δ peak of (MPA/Tetra Thiol)/TTT and (BMP/Tetra Thiol)/TTT films.

Table 2. Glass Transition Temperature for Thiol−Ene Networks as a Function of BMP and MPA Content

	BMP		MPA	
$[SH]_{Tetra\ Thiol}$:$[SH]_{Mono\ Thiol}$	DMA (°C)	DSC (°C)	DMA (°C)	DSC (°C)
100:0	64	49	64	49
95:5	55	39	63	45
90:10	48	35	58	38
80:20	32	18	50	33
65:35	10	−5	30	22

Table 3. Storage Modulus (E') in the Rubbery Region at T_g + 50 °C and Heat Capacity Change ($\triangle C_p$) at the Glass Transition for Thiol−Ene Networks as a Function of BMP and MPA Content

	E' (MPa)		$\triangle C_p$ (J/(g °C))	
$[SH]_{Tetra\ Thiol}$:$[SH]_{Mono\ Thiol}$	BMP	MPA	BMP	MPA
100:0	19.6	19.6	0.27	0.27
95:5	15.5	19.6	0.31	0.32
90:10	5.4	13.2	0.32	0.34
80:20	3.3	8.3	0.33	0.35
65:35	2.4	3.5	0.34	0.38

perature, pendulum hardness, and refractive index are higher. Next, a similar comparison is made between Tri Thiol/TTT, (BMP/Tetra Thiol)/TTT, and (MPA/Tetra Thiol)/TTT networks formed from mixtures with lower TAF. From Table 5, even when the TAF drops to 2.5, because of hydrogen bonding the (MPA/Tetra Thiol)/TTT network still has a T_g value similar to that of the Tri Thiol/TTT network, while the T_g of the (BMP/Tetra Thiol)/TTT network drops significantly as the TAF decreases to 2.5. Moreover, although the Persoz hardness of the (MPA/Tetra Thiol)/TTT network decreases by a little over a factor of 2, it still is much harder than the (BMP/Tetra Thiol)/TTT network (Persoz hardness of 37 s), which decreases by over a factor of 4 when TAF decreases from 3.0 to 2.5. The refractive index value change is also much larger for the (BMP/Tetra Thiol)/TTT network with a decrease in TAF from 3.08 to 2.50. From the results in Tables 4 and 5 it is quite apparent that hydrogen bonding can have a distinct effect on a base thiol−ene network matrix that can lead to properties that are equivalent to, or even better than, traditional thiol−ene network systems

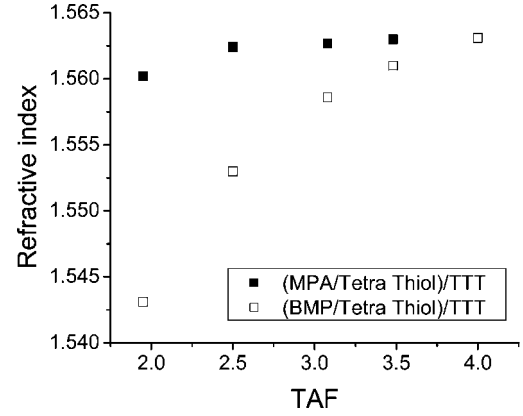

Figure 6. Refractive index as a function thiol average functionality (TAF) for (MPA/Tetra Thiol)/TTT and (BMP/Tetra Thiol)/TTT films.

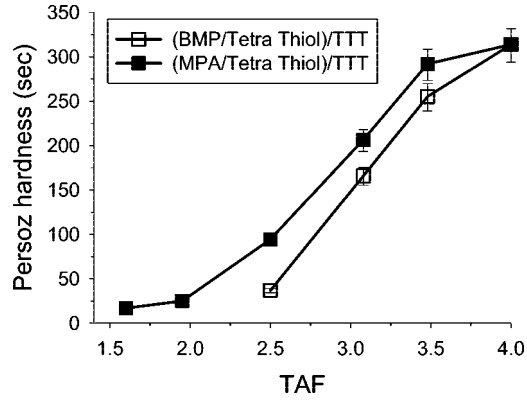

Figure 7. Persoz hardness as the function of thiol average functionality (TAF).

(i.e., the Tri Thiol/TTT) from mixtures with equal thiol functionality.

Next the amount of residual monomer and other impurities that can be extracted using a typical polar solvent such as acetonitrile is evaluated. As shown in Table 6, the gel fraction

Table 4. Property Comparison of Three Thiol−Ene Networks: Tri Thiol/TTT (TAF = 3), (BMP/Tetra Thiol)/TTT (TAF = 3.08), and (MPA/Tetra Thiol)/TTT (TAF = 3.08)

samples	Tri Thiol/TTT (TAF = 3.00)	(BMP/Tetra Thiol)/TTT (TAF = 3.08)	(MPA/Tetra Thiol)/TTT (TAF = 3.08)
T_g (°C)[a]	30	35	38
pendulum hardness (s)	168	167	208
refractive index	1.5561	1.5586	1.5627

[a] By DSC.

Table 5. Property Comparison of Three Thiol−Ene Systems: Tri Thiol/TTT (TAF = 3.00), (BMP/Tetra Thiol)/TTT (TAF = 2.50), and (MPA/Tetra Thiol)/TTT (TAF = 2.50)

samples	Tri Thiol/TTT (TAF = 3.00)	(BMP/Tetra Thiol)/TTT (TAF = 2.50)	(MPA/Tetra Thiol)/TTT (TAF = 2.50)
T_g (°C)[a]	30	18	33
pendulum hardness (s)	168	37	95
refractive index	1.5561	1.5530	1.5624

[a] By DSC.

Table 6. Gel Fraction of Thiol−Ene Networks as a Function of BMP and MPA Content

	gel fraction (%)[a]	
$[SH]_{Tetra\ Thiol}$:$[SH]_{Mono\ Thiol}$	BMP	MPA
100:0	99.7	99.7
95:5	99.5	99.8
90:10	99.1	99.6
80:20	98.2	98.9
65:35	93.5	95.9
50:50	80.4	84.5

[a] At 65 °C for 5 days in acetonitrile ($W_{after\ extraction}/W_{initial} \times 100$) where $W_{after\ extraction}$ is the weight of the thiol−ene network after extraction and $W_{initial}$ is the weight before extraction.

of all of the thiol−ene films is higher than 98%, except for the two films with the lowest TAF. This is certainly consistent with the higher monofunctional content in the two samples with lower TAF used to make the corresponding thiol−ene networks.

Thiol−ene networks, due to their unprecedented uniformity, can experience significant volume and enthalpy relaxation below the glass transition.[17] Analysis of isothermal enthalpy relaxation can provide a direct measure of the overall sub-T_g relaxation rate of polymer networks. As shown in Figure 8a,b, for all of the (MPA/Tetra Thiol)/TTT and (BMP/Tetra Thiol)/TTT photocured networks, there is extensive enthalpy relaxation after 60 min of physical aging at (T_g − 10) °C for each sample. For comparison, the results for unannealed samples are also given. Initially for both systems, as shown in Figure 9, enthalpy relaxation decreased with increasing TAF, consistent with the effect of network density of photopolymerized thiol−ene networks on enthalpy relaxation.[17] When TAF is 2.5 or greater where the connecting density of the polymer network is high, hydrogen bonding, which incorporates additional physical linkages into the thiol−ene polymer network, does not result in significant differences in the enthalpy relaxation between the (MPA/Tetra Thiol)/TTT and (BMP/Tetra Thiol)/TTT networks. In other words, the isothermal enthalpy for (MPA/Tetra Thiol)/TTT networks with TAF = 2.5, 3.0, and 3.5 is only a little higher than that for (BMP/Tetra Thiol)/TTT networks. However, when the nominal TAF decreases to 2 or less, and hence the connecting cross-link density due to covalent bonding is low or nonexistent, the effect of hydrogen bonding on the isothermal enthalpy relaxation is significant.

In order to more clearly define the role of hydrogen bonding on the sub-T_g physical aging process, the change in the isothermal enthalpy relaxation as a function of annealing time was evaluated. The systems with TAF = 1.95, for which the effect of hydrogen bonding is significant, were selected for this analysis. Both (MPA/Tetra Thiol)/TTT and (BMP/Tetra Thiol)/TTT films with TAF = 1.95 were annealed at (T_g − 10) °C for 0, 60, 120, 180, 300, 480, 720, and 1200 min. It is clear to see in Figure 10 that the 35:65 (MPA/Tetra Thiol)/TTT system attains a higher extent of enthalpy relaxation than the 35:65 (BMP/Tetra Thiol)/TTT system for the time period evaluated. The higher enthalpy relaxation for the 35:65 (MPA/Tetra Thiol)/TTT network compared to the 35:65 (BMP/Tetra Thiol)/TTT network is in accordance with the results for a linear polymer obtained by Cowie et al., who reported that excess enthalpy initially is locked into unfavorable configurations by thermoreversible hydrogen bonding of interacting acid groups.[18]

An additional effect of hydrogen bonding is the heat capacity change (ΔC_p) at T_g which has been correlated to differences in enthalpy relaxation.[18−20] Thermally reversible noncovalent interactions such as hydrogen bonding or dipole−dipole result in larger changes in heat capacity through the thermal transitions of polymers because of the larger increase in conformational degree of freedom for the system.[21] From the basic DSC scans for both MPA/Tetra Thiol)/TTT and (BMP/Tetra Thiol)/TTT networks, we also calculated the heat capacity differences between the glassy and rubbery states (Table 3). These results complement the results in Figure 10 and are consistent with the results for copolymers of styrene and *p*-hydroxystyrene and other related comonomers which readily form hydrogen-bonded structures.[18] The higher ΔC_p values are greater in each case for the (MPA/Tetra Thiol) networks than the (BMP/Tetra Thiol) networks due to greater available conformational freedom in the rubbery state which becomes accessible by breaking thermally reversible hydrogen bonding with increasing temper-

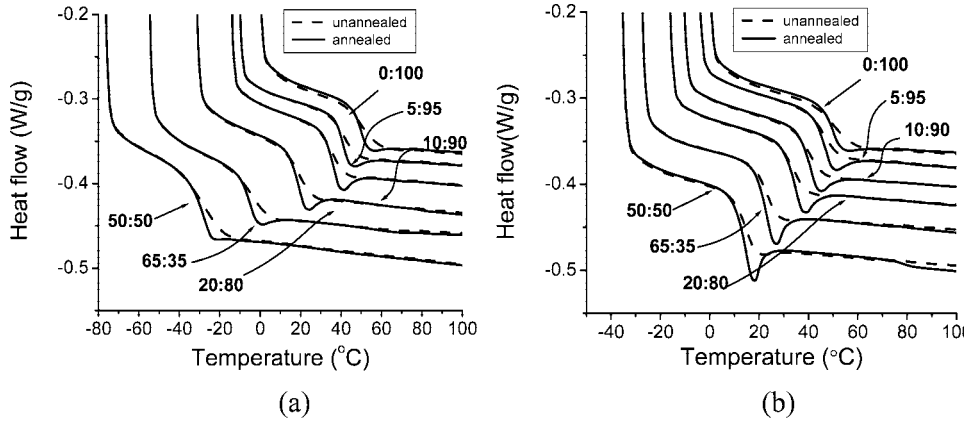

Figure 8. DSC curves for (a) (BMP/Tetra Thiol)/TTT and (b) (MPA/Tetra Thiol)/TTT networks.

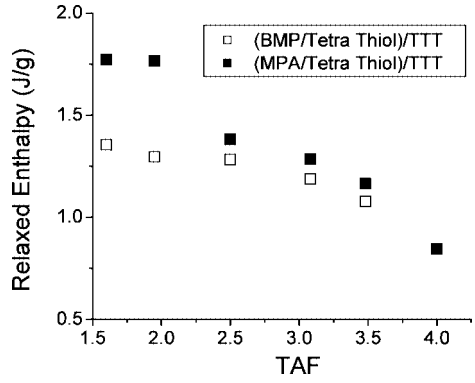

Figure 9. Isothermal enthalpy relaxation as a function of thiol average functionality (TAF).

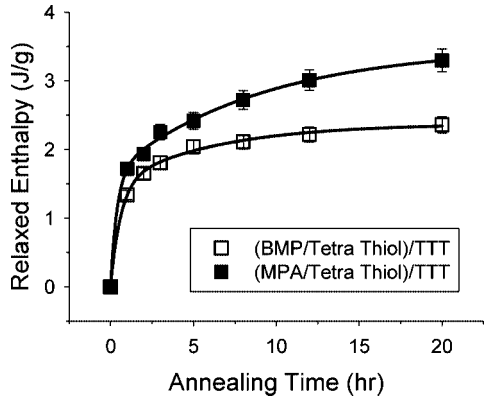

Figure 10. Isothermal enthalpy relaxation as a function of time at temperature of (T_g − 10) °C for both (MPA/Tetra Thiol)/TTT and (BMP/Tetra Thiol)/TTT films with thiol average functionality (TAF) at 1.95.

ature, resulting in a larger difference in the extent of isothermal enthalpic relaxation.

Conclusions

The effect of hydrogen bonding on both the kinetics and physical properties for two thiol−ene systems, (BMP/Tetra Thiol)/TTT and (MPA/Tetra Thiol)/TTT, has been investigated. Hydrogen bonding in the thiol−ene network containing MPA leads to enhanced glass transition temperatures, refractive index, and hardness compared to comparable networks formed using BMP. In addition, storage moduli above the glass transition are higher where hydrogen bonding occurs. It has also been demonstrated that sub-T_g annealing results in a higher extent of enthalpy relaxation for the hydrogen-bonded thiol−ene network system ((MPA/Tetra Thiol)/TTT), similar to what has been reported in the past for linear polymers. The thiol−ene networks are inherently very highly uniform networks and hence provide an ideal opportunity for evaluating physical and chemical structural effects on network properties. Accordingly, the results presented herein provide a clear picture of how hydrogen bonding can, in general, affect physical and mechanical properties of networks. The use of thiol−ene networks as a basic platform for assessing other chemical and structural effects on physical and optical properties will be the subject of future investigations.

Acknowledgment. We thank Bruno Bock Chemische Fabrik GmbH & Co. KG and Ciba Specialty Chemicals for materials and Fusion UV Systems for the lamp system.

References and Notes

(1) Coleman, M. M.; Painter, P. C. *Prog. Polym. Sci.* **1995**, *20*, 1.
(2) Jiang, M.; Li, M.; Xiang, M.; Zhou, H. *Adv. Polym. Sci.* **1999**, *146*, 121.
(3) Song, T.; Goh, S. H.; Lee, S. Y. *Macromolecules* **2002**, *35*, 4133.
(4) Park, Y.; Veytsman, B.; Coleman, M.; Painter, P. *Macromolecules* **2005**, *38*, 3703.
(5) Mattia, J.; Painter, P. *Macromolecules* **2007**, *40*, 1546.
(6) Jansen, J. F. G. A.; Dias, A. A.; Dorschu, M.; Coussens, B. *Macromolecules* **2003**, *36*, 3861.
(7) Beckel, E. R.; Berchthold, K. A.; Nie, J.; Lu, H.; Stansburry, J. W.; Bowman, C. N. *Polym. Prepr.* **2003**, *44*, 31.
(8) Berchthold, K. A.; Nie, J.; Stansburry, J. W.; Hacioglu, B.; Beckel, E. R.; Bowman, C. N. *Macromolecules* **2004**, *37*, 3165.
(9) Lee, T. Y.; Roper, T. M.; Jönsson, E. S.; Guymon, C. A.; Hoyle, C. E. *Macromolecules* **2004**, *37*, 3659.
(10) Zhou, H.; Li, Q.; Lee, T. Y.; Guymon, C. A.; Jönsson, E. S.; Hoyle, C. E. *Macromolecules* **2006**, *39*, 8269.
(11) Cramer, N. B.; Bowman, C. N. *Polym. Prepr.* **2003**, *44*, 17.
(12) Hoyle, C. E.; Lee, T. Y.; Roper, T. *J. Polym. Sci., Part A: Polym. Chem.* **2004**, *42*, 5301.
(13) Li, Q.; Zhou, H.; Wicks, D. A.; Hoyle, C. E. *J. Polym. Sci., Part A: Polym. Chem.* **2007**, *45*, 5103.
(14) Huang, Y.; Paul, D. R. *Macromolecules* **2006**, *39*, 1554.
(15) Jacobine, A. F.; Glaser, D. M.; Grabek, P. J.; Mancini, D.; Masterson, M.; Nakos, S. T.; Rakas, M. A.; Woods, J. G. *J. Appl. Polym. Sci.* **1992**, *45*, 471.
(16) Chiou, B.; Khan, S. *Macromolecules* **1997**, *30*, 7322.
(17) Shin, J.; Nazarenko, S.; Hoyle, C. E. *Macromolecules* **2008**, *41*, 6741.
(18) McGonigle, E. A.; Cowie, J. M. G.; Arrighi, V.; Pethrick, R. A. *J. Mater. Sci.* **2005**, *40*, 1869.
(19) Hutchinson, J. M.; Kumar, P. *Thermochim. Acta* **2002**, *391*, 197.
(20) Huang, D.; Yang, Y.; Zhuang, G.; Li, B. *Macromolecules* **1999**, *32*, 6675.
(21) Cooper, A. *Biophys. Chem.* **2000**, *85*, 25.

MA802645J